Planar temperature sensing using heavy-metal-free quantum dots with micrometer resolution

2014 Nanotechnology 25 285501

(http://iopscience.iop.org/0957-4484/25/28/285501)

IOP Publishing Nanotechnology
Nanotechnology **25** (2014) 285501 (8pp) doi:10.1088/0957-4484/25/28/285501

Planar temperature sensing using heavy-metal-free quantum dots with micrometer resolution

Wenyan Liu[1], Yu Zhang[1,2], Hua Wu[1], Yi Feng[2], Tieqiang Zhang[2], Wenzhu Gao[2], Hairong Chu[3], Jingzhi Yin[1], Tian Cui[2], Yiding Wang[1], Jun Zhao[4,5] and William W. Yu[1,4,5]

[1] State Key Laboratory of Integrated Optoelectronics, and College of Electronic Science and Engineering, Jilin University, Changchun 130012, People's Republic of China
[2] State Key Laboratory of Superhard Materials and College of Physics, Jilin University, Changchun 130012, People's Republic of China
[3] Changchun Institute of Optics, Fine Mechanics, and Physics, Chinese Academy of Sciences, Changchun 130025, People's Republic of China
[4] College of Material Science and Engineering, Qingdao University of Science and Technology, Qingdao 266042, People's Republic of China
[5] Department of Chemistry and Physics, Louisiana State University, Shreveport, LA 71115, USA

E-mail: yuzhang@jlu.edu.cn and wyu6000@gmail.com

Received 10 February 2014, revised 10 May 2014
Accepted for publication 20 May 2014
Published 27 June 2014

Abstract

This work describes a micrometer resolution and plane-array temperature-sensing method using the photoluminescence (PL) of ZnCuInS/ZnSe/ZnS quantum dots (QDs). Heavy-metal-free QDs were directly deposited on a printed circuit board to analyze the surface temperature of the devices on the board. An optical fiber monochromator and a high-powered microscope were employed to fabricate a system which could collect temperature-dependent QD emissions from the micrometer area for the temperature measurements. This system realizes the imaging of the surface temperature distribution in the planar micrometer area. Temperature sensitivity of the PL intensity reached 0.66% $°C^{-1}$, and the relative error was less than 2%.

Keywords: temperature sensing, micrometer resolution, planar, ZnCuInS/ZnSe/ZnS, quantum dots

(Some figures may appear in colour only in the online journal)

1. Introduction

With the development of integrated circuits (ICs) and micro/nano-electromechanical systems (MEMS/NEMS), it is very important to analyze and monitor the performance of these micro-/nano-scale systems. In many of these applications, temperature plays an important role in overall chip performance. For example, the performance uniformity of each single chip in an alternating current/high voltage (AC/HV) LED is an important factor affecting a device's lifetime and can be analyzed by using surface temperature. The junction temperature,another critical parameter that affects internal efficiency, maximum output power, reliability, and other specifications of LEDs, can also be analyzed by usin surface temperature [1]. Temperature measurement is also an effective way to detect defects in MEMS/NEMS and ICs [2].

Because of the low spatial resolution, measuring the temperature of MEMS/NEMS and ICs by using conventional techniques becomes extremely challenging either in the contact or noncontact modes when the characteristic dimension of the functional structures reduces down to the nanometer range [2–4]. Traditional temperature measurement methods such as contact measurement of thermocouples and noncontact measurement of thermal infrared imagers suffer similar limitations [5–8]. Furthermore, these methods are limited to single-spot data acquisition, and the complexity of

the assembly (fabrication) is increased when thermocouples are incorporated [4].

Luminescent semiconductor quantum dots (QDs) have been considered for use as temperature sensing material on microchips because of properties such as strong confinement in all three spatial dimensions [9], broad absorption and tunable emission [2, 10], small size (a few nanometers) [11], and easy chemical modification and processing [12]. Because QDs can be directly placed into micro-/nano-channels for temperature measurement through far-field optical readouts, more and more researchers have paid attention to QD-based temperature sensing systems.

Previous works have shown that the spectroscopic characteristics for an ensemble of CdSe QDs shift with temperature [13–16]. Therefore, CdSe QDs were integrated into micro- and nano-structures to monitor surface temperatures with a spectral shift sensitivity of 0.1 nm $°C^{-1}$ [2]. Also, the temperature-dependent optical spectra of PbSe QDs have been confirmed as having a better sensing sensitivity of 0.16 nm $°C^{-1}$ [10], and they have been employed as real-time and on-chip temperature sensors to monitor the surface temperature of GaN LED chips [17]. The optical spectra of CdTe QDs have been used for temperature sensing with a temperature coefficient of 1.47% $°C^{-1}$ [18]. Though the use of these QDs in temperature sensing is promising, a serious drawback is their toxic heavy metal components of cadmium and lead, which raise concerns about carcinogenicity and other chronic health risks as well as disposal hazards [19].

In this paper we propose the use of non-toxic ZnCuInS/ZnSe/ZnS QDs for temperature sensing by employing temperature-dependent far-field optical readouts. In our work, we demonstrated the feasibility of directly depositing a film of QDs on a printed circuit board (PCB) for noncontact, local temperature sensing of IC and MEMS. We did so by designing a calibrated PL spectra-based sensing system that included an optical fiber monochromator, a high-power microscope, and a fine wheel structure. This plane-array and micrometer resolution temperature-sensing system may be promising in detecting defects and sensing micro-/nano-scale temperatures.

2. Experimental section

2.1. Chemicals

Indium (III) iodide (InI_3, 99.99%) and selenium powder (Se, 100 meshes) were purchased from Alfa Aesar. Coppor (I) iodide (CuI, 98%), dichlorodiphenyltrichloroethane (DDT, 98%), tributylphosphine (TBP, 95%), diethyldithiocarbamic acid zinc (DECZn, 98%), zinc oxide (ZnO, 99.99%),1-octadecene (ODE, 90%), and oleylamine (OAm, 80%–90%) were obtained from Aladdin. Acetone, methanol, hexane, and toluene were purchased from Sigma-Aldrich. All chemicals were used directly without further treatment.

2.2. Precursor solution

0.181 g DECZn was dissolved in 6 mL TBP and 24 mL ODE and degassed for 20 min. Then, the mixed solution was heated to 70 °C for 30 min to obtain a DECZn/TBP/ODE solution. 0.0857 g CuI and 0.113 g InI_3 were respectively placed in 10 mL OAm under sonication until two clear solutions were obtained. 0.078 g Se powder was dissolved into 10 mL TBP at room temperature to get a clear solution. 0.100 mg ZnO and 2.073 g OA were added to 10 ml ODE at 200 °C under N_2 flow to obtain a colorless zinc oleate/ODE solution.

2.3. Synthesis

The ZnCuInS/ZnSe/ZnS QDs were synthesized by using an approach modified from the method proposed by Uehara *et al* [20] and Tan *et al* [21]. In a typical synthesis of 2.3 nm QDs, 2 mL CuI/OAm, 2 mL InI_3/OAm, and 6 mL DECZn/TBP/ODE solutions were mixed into 20 mL ODE (which had been degassed with N_2 for 10 min) under N_2. The mixture was heated at 70 °C for 30 min and then at 120 °C for 4 h. 2 mL Se/TBP and 2 mL zinc oleate/ODE solutions were then added dropwise into the solution just describes.

Ten min later, another 2 mL Se/TBP and 2 mL zinc oleate/ODE solutions were dripped into the reaction solution and the temperature was increased to and maintained at 180 °C for 1 h. After that, the reaction temperature was adjusted back to 150 °C for another 1 h. Then 3 mL DECZn/TBP/ODE solution was added to the flask, and the reaction solution was heated to and maintained at 210 °C for 30 min. At this time the temperature was again set back to 150 °C for annealing (2 h). The solution was further cooled to 100 °C, and 3 mL DDT was added. After 1 h, the solution was cooled to room temperature. The growth temperatures were maintained at 210 °C and 180 °C to achieve particle sizes of 3.3 nm and 2.7 nm, respectively.

The QD solution was mixed with an equal volume of hexane solution and then extracted once with twice the volume of methanol. The QDs were further precipitated by twice the volume of methanol and an equal volume of acetone [22–24]. The purified ZnCuInS/ZnSe/ZnS QDs were finally dispersed in toluene for further research.

2.4. Characterization

Absorption spectra were measured on a Perkin-Elmer Lambda 950 UV-Vis spectrophotometer. Photoluminescence (PL) spectra were recorded on a Perkin-Elmer LS50B spectrophotometer. Transmission electron microscopy (TEM) studies were performed by using a TECNAI F30ST TEM operated at 300 kV. Samples for TEM were

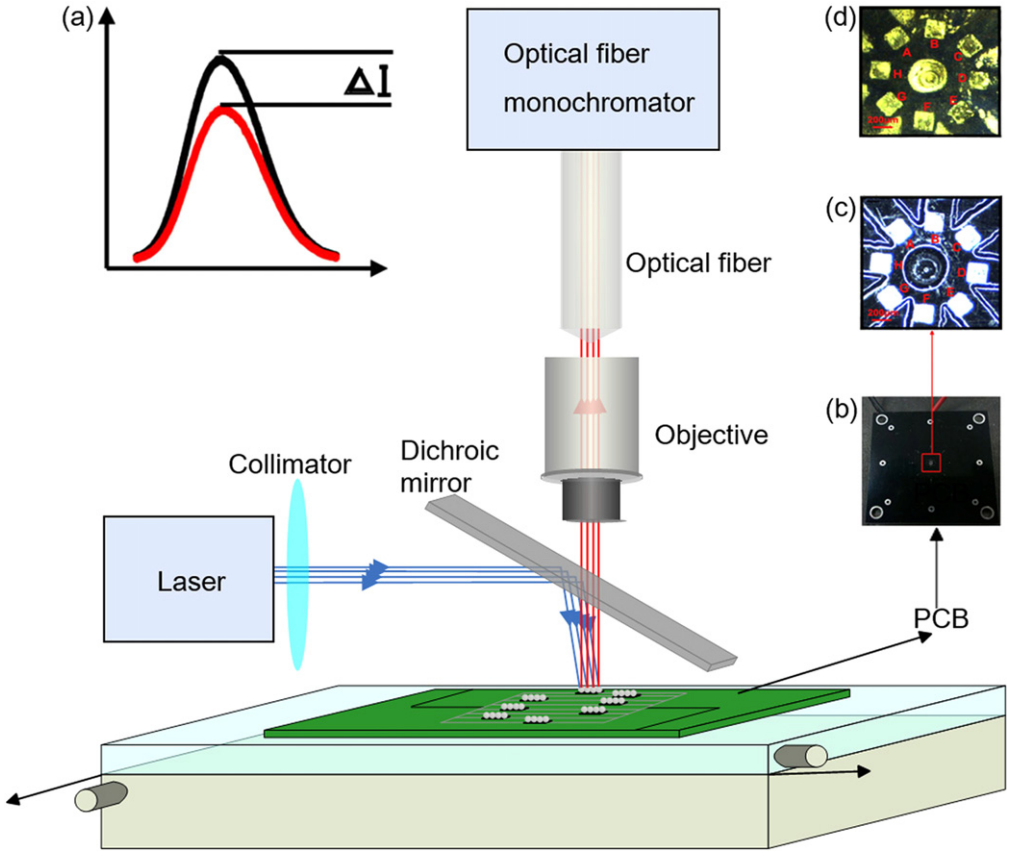

Figure 1. Schematic diagram of noncontact temperature characterization system using QDs (a). Image of PCB (b) and enlarged images of PCB without QDs (c) and with QDs (d). A–H are eight micrometer-sized resistors.

prepared by placing a 4 μL toluene solution of nanocrystals on copper grids coated with ultrathin carbon film in a glove box.

3. Results and discussion

3.1. Detecting system

Figure 1 shows the schematic diagram of the ZnCuInS/ZnSe/ZnS QDs-based temperature sensing system. The QD solution was spread on the surface of the PCB and then dried under air. The sample was mounted on a sample holder with a moving accuracy of 1 μm. QDs on the surface of samples were excited by a 450 nm continuous-wave laser with a collimator.

The temperature-related emission of QDs in the region of $1 \times 1\ \mu m^2$ was collected by the microscope system with an objective lens (10×) and an optical fiber (with a core diameter of 10 μm). The emission from QDs was collected through a dichroic mirror. After a circuit board or an electronic device coated with QDs is placed on the sample holder, the holder will shift along the pixels one by one to record the spectrum and to analyze the temperature and surface properties of the device. The spectra of each point on the device were scanned twice, once before and once during operation. Then the spectra before operation were considered as '1' and the relative intensity was obtained for temperature calibration and calculation.

3.2. Temperature-dependent emission property

Figure 2 displays the optical absorption, PL spectra, and temperature-dependent PL for three sizes of ZnCuInS/ZnSe/ZnS core/shell/shell QDs dissolved in toluene. The Stokes shifts determined from figure 2 were 398.6, 436.7, and 460 meV. The insets in figures 2(a)–(c) show the TEM images of ZnCuInS/ZnSe/ZnS QDs with particle sizes of 3.3, 2.7, and 2.3 nm.

The 2.3 nm QDs were employed as a temperature sensor as an example. The quantum yields (QYs) of the ZnCuInS/ZnSe/ZnS QDs were 57% in solution and 8% as a thin film measured with an integrating sphere. The ZnCuInS/ZnSe/ZnS QDs have similar temperature-dependent PL properties for different particle sizes [25]. To further confirm the spectra stability of the QDs, three cyclic tests of the change of temperature-dependent PL intensity were measured as shown in figure 3(a). The PL intensity decreases with increasing temperature and can return to its original spectrum when the material is cooled. The good reversibility of PL intensity was observed for the second and third cycles of heating and cooling. The PL intensity was able to return to its original

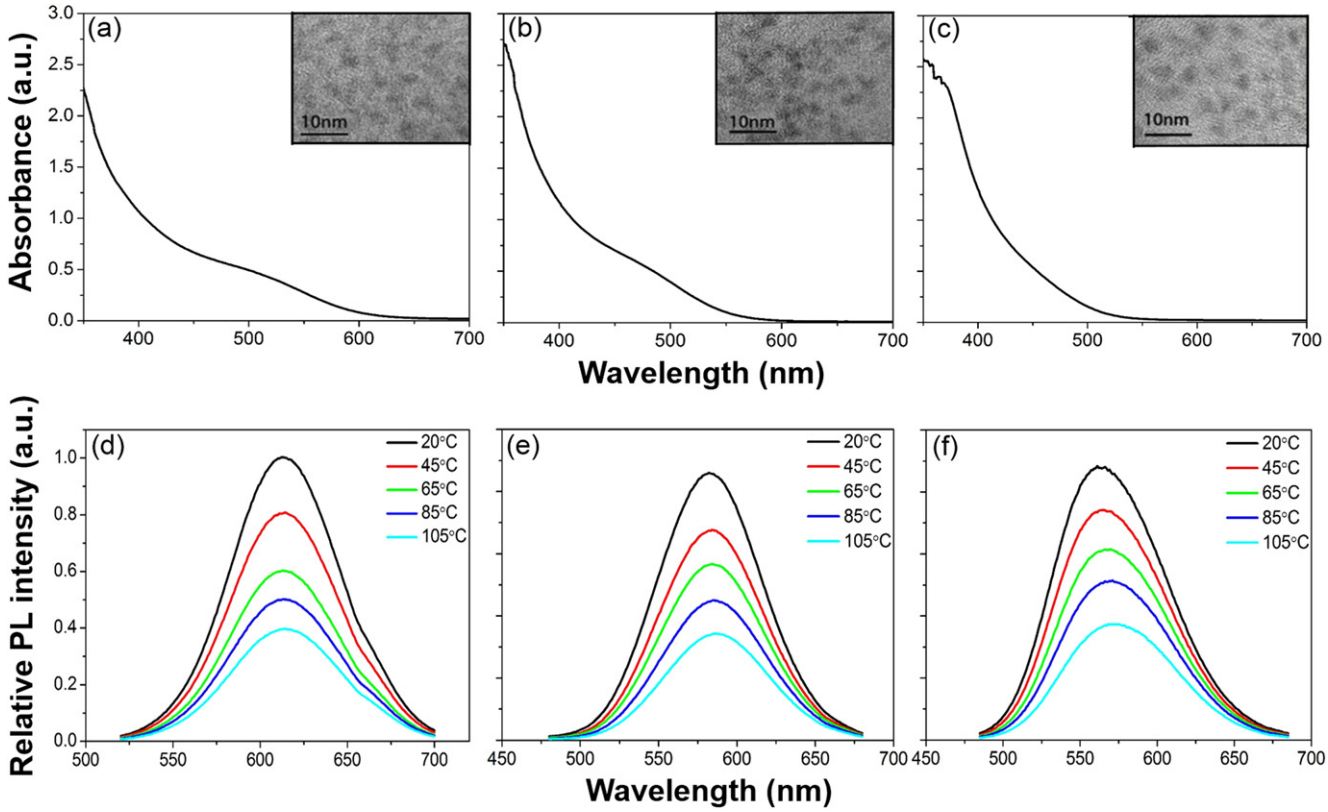

Figure 2. Absorption spectra and TEM images of ZnCuInS/ZnSe/ZnS QDs: 3.3 nm (a), 2.7 nm (b), and 2.3 nm (c). Temperature-dependent PL spectra of 3.3 nm (d), 2.7 nm (e), and 2.3 nm (f) from 20 °C to 105 °C.

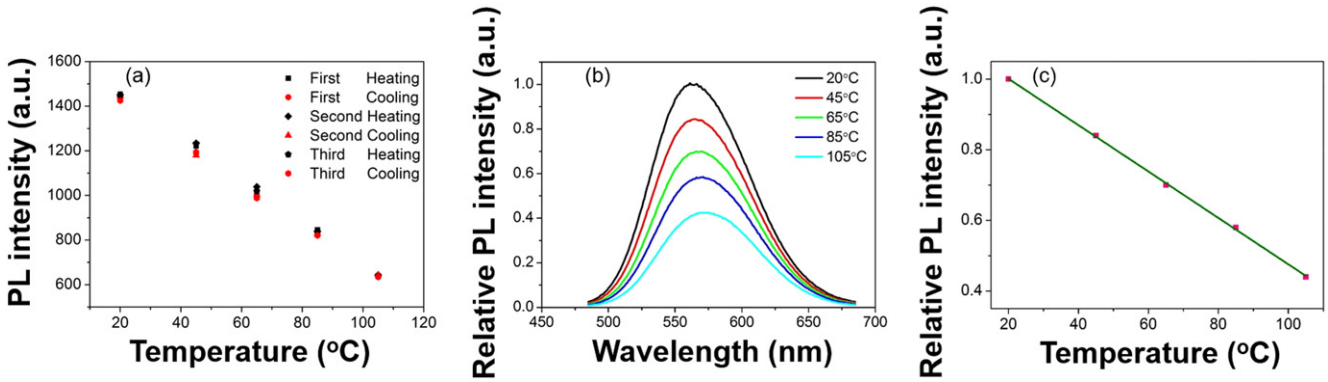

Figure 3. Three cycles of the reversible change of temperature-dependent PL intensity for ZnCuInS/ZnSe/ZnS QDs (a). Normalized PL spectra of ZnCuInS/ZnSe/ZnS QDs at temperatures of 20 °C to 105 °C (b). The calibrating curve of the normalized PL intensity for temperature from 20 °C to 105 °C (c).

values after three cycles of heating and cooling at the related temperature. Such good reversibility ensures that this material is appropriate for repeated temperature measurements.

Because the PL origin of ZnCuInS/ZnSe/ZnS QDs is most probably due to the recombination of a quantized conduction-band state to a localized intra-gap state and the donor and acceptor pair [25–28], the temperature-dependent band gap shifts of these QDs were not as strong as that of band-edge emitting material. Therefore, the PL intensity (not the peak position) was employed in this system. However, the PL intensity on the surface of the device varies with the number of QDs, and it is difficult to control the uniformity of the QD film; therefore, the normalized intensity of PL spectra was proposed to be capable of simplifying the temperature sensing.

We used room temperature (20 °C) as the reference temperature. Before the measurement, we scanned the optical spectrum of each pixel at room temperature, recorded the PL intensity, and normalized it at 1.0 for an individual pixel. Then we scanned the surface pixel emission again when the circuit board or electronic device coated with QDs was operating. According to this strategy, all the operating emissions were compared with the PL intensity at room temperature. The processed result is shown in figure 3(b). The temperature coefficient of PL intensity was thus obtained as

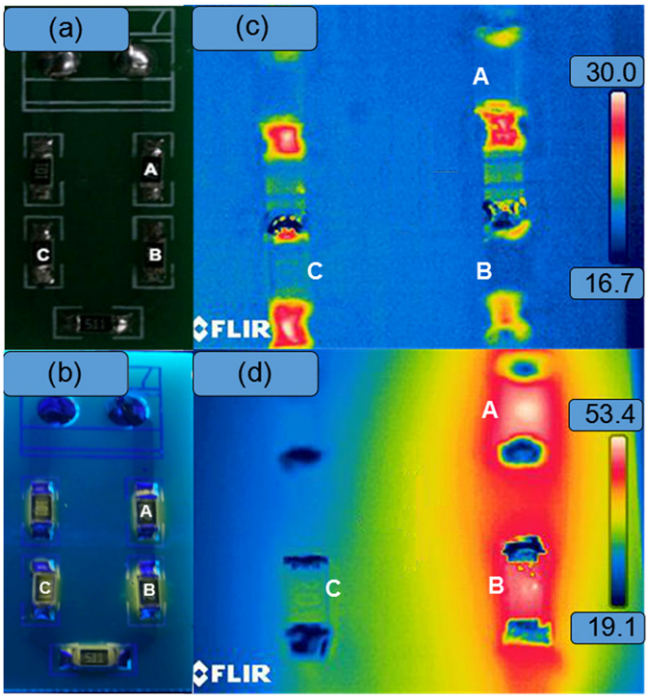

Figure 4. Images of PCB without QDs (a) and with QDs under UV lamp (b). Thermal infrared images of PCB with QDs operated at 0 mA (c) and 7.9 mA (d). A, B, and C are three resistors in a series circuit.

0.66% $°C^{-1}$, which was decent compared with those of CdSe (~0.34% $°C^{-1}$) and CdTe QDs (~1.47% $°C^{-1}$) [2, 18]. The PL intensity comparison (normalization) demonstrates that the concentration of the QDs (number of QD particles) and the nonuniformity of QD film on the PCB will not affect the detecting results, which makes this method simple to use.

Before measuring the temperature of the QD film, a standard curve of temperature-dependent normalized PL intensity is needed for calibration. Figure 3(c) shows the standard line of temperature-dependent PL intensity of 2.3 nm QDs from 20 °C to 105 °C. The calibration equation was derived as,

$$I_n = 1.136 - 0.00657 \times t \quad (1)$$

where I_n is the normalized PL intensity and t is the temperature (°C). As can be seen from figure 3(c), intensity decreases linearly as temperature increases. According to the equation, temperature can be calculated through the normalized PL intensity of ZnCuInS/ZnSe/ZnS QD film.

3.3. Temperature measurement on PCB

First, a series circuit composed of five different resistors was employed to analyze the effectiveness of our temperature-detecting system. A stable current was applied to the series resistors. Figures 4(a) and (b) show the five resistors; three of them have resistances of 1982 Ω (A), 992 Ω (B) and 196 Ω

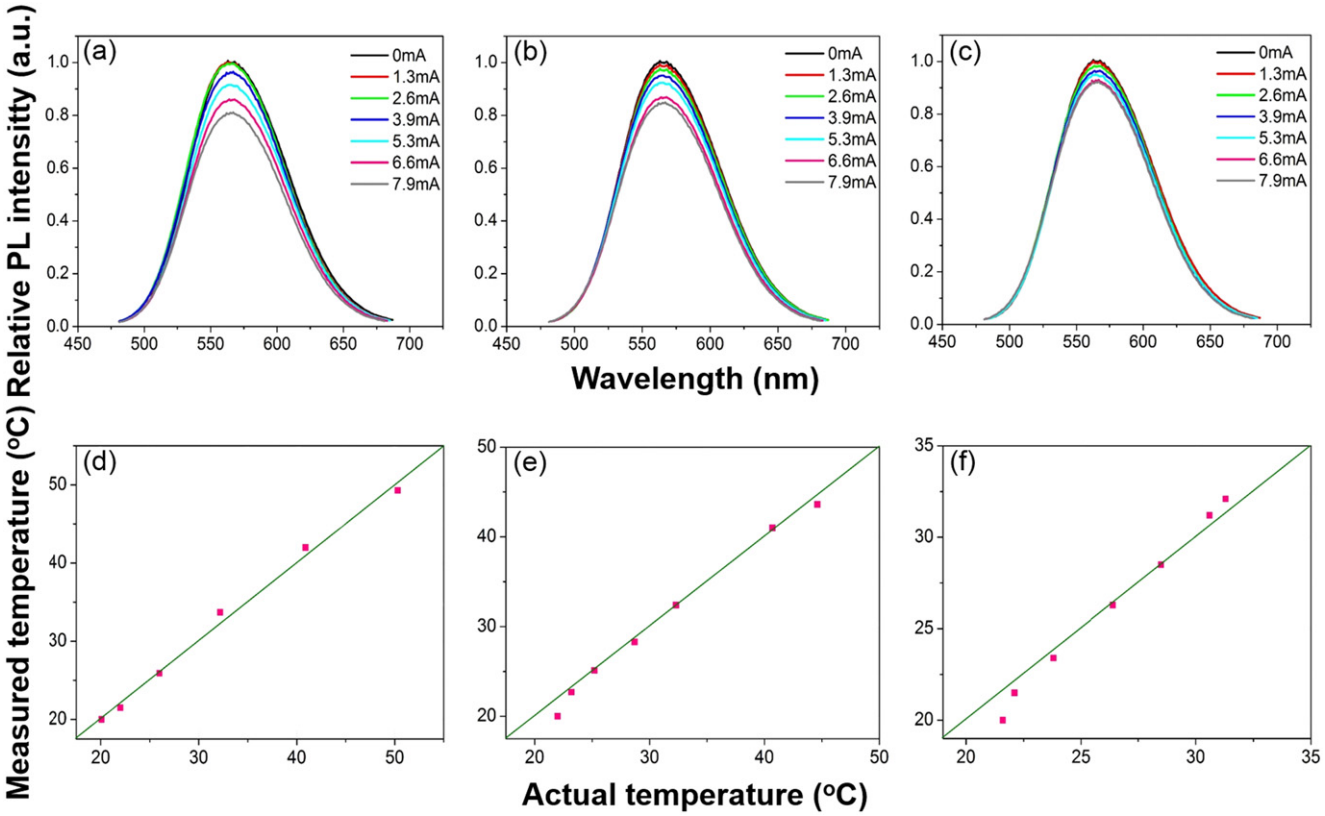

Figure 5. PL intensity of QD film with increasing biases of resistors A (a), B (b), and C (c) (see figure 4). Comparison of QD-measured temperature (vertical axis) achieved from QD sensors and temperature (horizontal axis) achieved from thermal infrared imager for resistors A (d), B (e), and C (f).

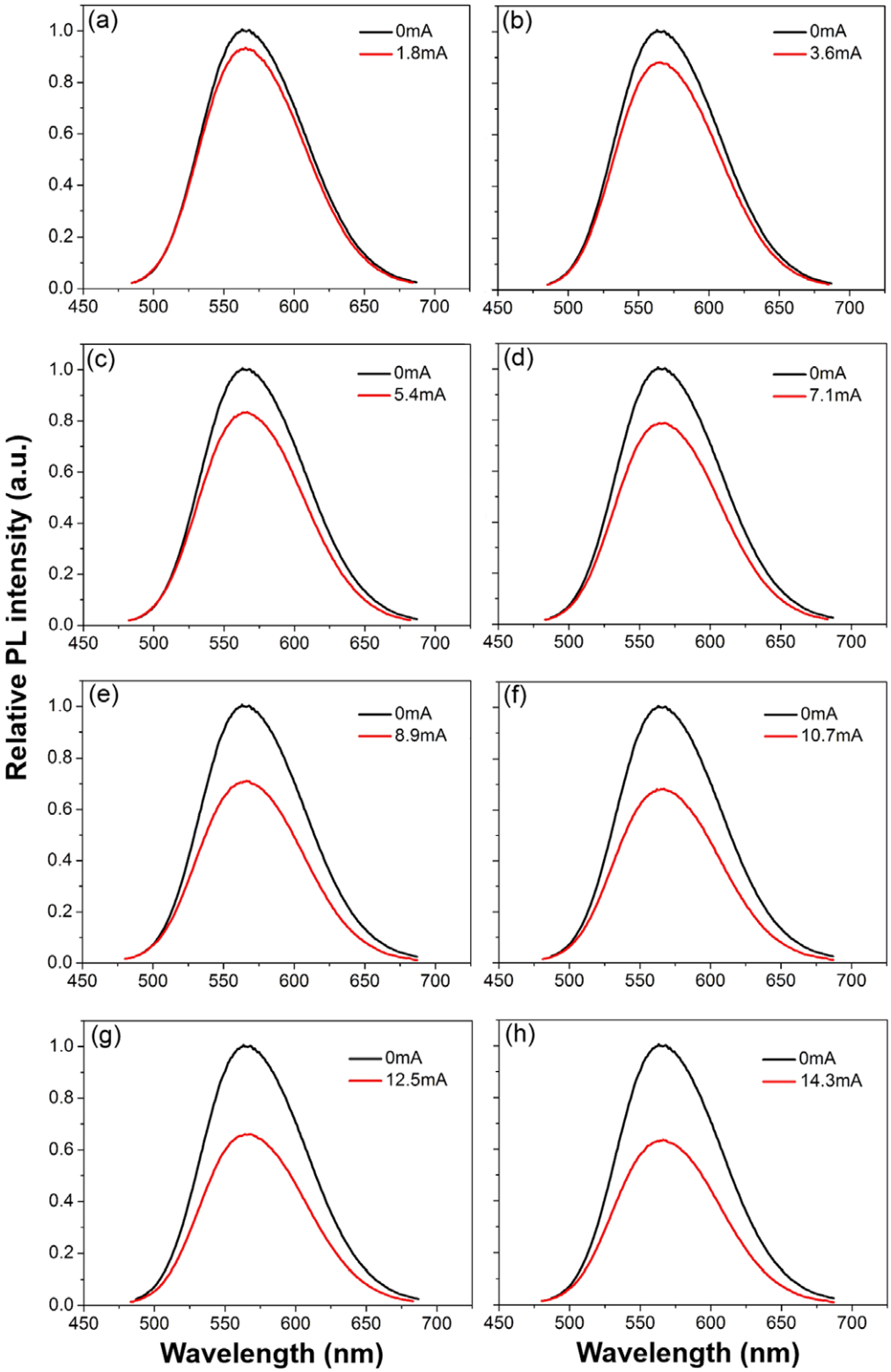

Figure 6. PL spectra of eight micrometer resistors A (a), B (b), C (c), D (d), E (e), F (f), G (g), and H (h) operating at different currents (see figure 1).

(C), respectively. Each resistor has a surface area of $5 \times 3\ \text{mm}^2$. The ZnCuInS/ZnSe/ZnS QDs were spread on the surface of the resistors. Figure 4(a) is the image of the PCB without QDs and figure 4(b) shows the image of the PCB with QDs under a UV lamp. All the resistors operated at the same current but with different resistances, so the stabilized temperature for each resistor was different. The QD-covered PCB board was placed under an optical microscope with an

excitation light beam focused on it. The PL spectra of the QD films were thus collected for temperature measurement.

The spectral data were collected after the PCB operated for several minutes when the surface temperature reached equilibrium (no more changes). Figures 5(a)–(c) show the PL spectra of QDs on the three different resistors A, B, and C, respectively. The PL intensity at a current of 0 mA (room temperature) was used as the reference to achieve the normalized PL spectra at different currents. The PL intensity of the QD films decreased with the increased current and accordingly the increased temperature of the resistors.

According to the measured normalized PL intensity and equation (1), the surface temperatures of the resistors at different currents could be obtained. To analyze the accuracy of this temperature measurement, a thermal infrared imager was employed to monitor the surface temperature of the three resistors as a comparison. The images of the PCB obtained from the thermal infrared imager are given in figure 4 when the PCB was operating at 0 mA and 7.9 mA. The different colors indicate that the different resistors induced different surface temperatures. With the temperature increasing, the color varies from blue, green, yellow, and red to white. The comparison of the actual temperatures measured by the thermal infrared imager and the QD-measured temperatures for the three resistors are shown in figures 5(d)–(f). The relative error of the QD temperature system was 1.9%.

3.4. Plane array and micrometer-area temperature sensing

We also used a QD temperature sensor to analyze plane array and micrometer area circuits. The thermal infrared imager could no longer be used easily and directly to measure micrometer areas [7, 8]. The micrometer area circuits and systems were made of a black PCB with eight micrometer-sized resistors (with the same resistance) as shown in figures 1(c) and (d). The size of the micrometer resistors was $200 \times 200\ \mu m^2$.

When the resistors wereoperating, the currents in them differed and thus different surface temperatures were generated. ZnCuInS/ZnSe/ZnS QDs were spread on the surface of these resistors. A microscope with a spectrophotometer was employed to focus on one single device area at a time and collected the QD emission for each resistor. The circuit board was placed on the objective table. Through the movement of the objective table, the PL spectra of QD film on every resistor (no current) were respectively recorded as the reference and each PL intensity was set to be 1.0. The PL spectra of QD film on the resistors were then measured when the resistors had been operating for 10 min (that is, they had already reached temperature equilibrium with the surroundings). According to the normalized PL intensity of the QD film, the surface temperature of each resistor could be calculated according to equation (1).

The normalized PL spectra of the eight resistors are shown in figures 6(a)–(h). Therefore, the surface temperatures of the eight resistors can be determined by the relative PL intensity of the QDs film. The data for the measured temperatures of the resistors operating at different currents are shown in figure 7.

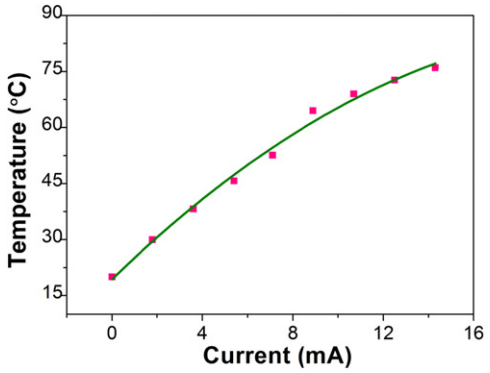

Figure 7. Resistor operating temperature measured by QDs at different currents.

To further determine the resolution of this temperature analysis system, we recorded the emission intensity of QDs on resistor H for an area of $200 \times 140\ \mu m^2$ as shown in figure 8(a). The color varied on the basis of the detected temperature for the surface of resistor H, which shows that this method can be used to analyze planar surface temperature with a $10 \times 10\ \mu m^2$ resolution, as shown in figure 8(b). This method can be applied to the analysis of a plane-array with micrometer resolution temperature detection, which is promising for use in detecting defects in highly integrated devices such as ICs. Defects and non-uniform distribution of cabling often occur in ICs in the form of broken diodes and cabling with different widths, which can cause different resistances or distributions of surface temperature while the IC is operating. Therefore, coating the device surface with a thin layer of the proposed QDs will show a detailed thermal image of the device so that one can directly find the broken point or non-uniform distribution.

4. Conclusions

We have described the application of ZnCuInS/ZnSe/ZnS core/shell/shell QDs as temperature sensors, which is made possible by their temperature-dependent PL intensity. We used the system we designed to analyze micro-area surface temperature with micrometer resolution and low analysis error.

Acknowledgments

This work was financially supported by the National Science Fund for Distinguished Young Scholars (61225018), the National 863 Program (2011AA050509), the National Natural Science Foundation of China (61106039, 51272084, 61306078), the National Postdoctoral Foundation (2011049015), the Jilin Province Key Fund (20140204079GX), the Hong Kong Scholar Program (XJ2012022), the Shandong Natural Science Foundation

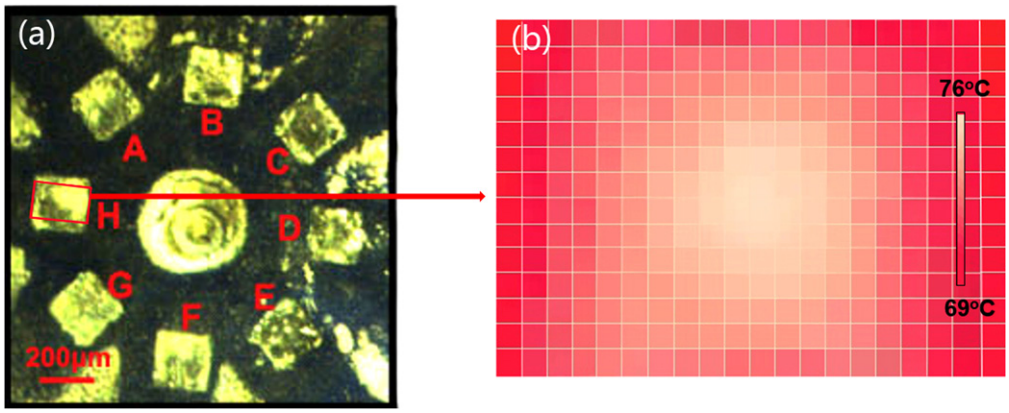

Figure 8. Image of micrometer-sized resistors on PCB with QDs (a) (also see figure 1(d)) and the surface temperature image of resistor H by QDs (b). The total area in (b) is $200 \times 140\ \mu m^2$, where each small square is $10 \times 10\ \mu m^2$.

(ZR2012FZ007), the State Key Laboratory of Integrated Optoelectronics (Jilin University, IOSKL2012ZZ12).

References

[1] Xi Y and Schubert E F 2004 *Appl. Phys. Lett.* **85** 2163–5
[2] Li S, Zhang K, Yang J, Lin L and Yang H 2007 *Nano Lett.* **7** 3102–5
[3] Jorez S, Laconte J, Cornet A and Raskin J-P 2005 *Meas. Sci. Technol.* **16** 1833–40
[4] Zhou J H, Yan H, Zheng Y Z and Wu H K 2009 *Adv. Funct. Mater.* **19** 324–9
[5] Khandurina J, McKnight T E, Jacobson S C, Waters L C, Foote R S and Ramsey J M 2000 *Anal. Chem.* **72** 2995–3000
[6] Kopp M U, de Mello A J and Manz A 1998 *Science* **280** 1046–8
[7] Bower S M, Kou J and Saylor J R 2009 *Rev. Sci. Instrum.* **80** 095107–13
[8] Tokunaga T, Narushima T, Yonezawa T, Sudo T, Okubo S, Komatsubara S, Sasaki K and Yamamoto T 2012 *J. Electron Microsc.* **61** 223–7
[9] Dawson P, Rubel O, Baranovskii S D, Pierz K, Thomas P and Göbel E O 2005 *Phys. Rev.* B **72** 235301–10
[10] Dai Q, Zhang Y, Wang Y, Hu M, Zou B, Wang Y and Yu W W 2010 *Langmuir* **26** 11435–40
[11] Kumar S, Jones M, Lo S S and Scholes G D 2007 *Small* **3** 1633–9
[12] Konstantatos G, Howard I, Fischer A, Hoogland S, Clifford J, Klem E, Levina L and Sargent E H 2006 *Nature* **442** 180–3
[13] Walker G W, Sundar V C, Rudzinski C M, Wun A W, Bawendi M G and Nocera D G 2003 *Appl. Phys. Lett.* **83** 3555–7
[14] Valerini D, Creti A, Lomascolo M, Manna L, Cingolani R and Anni M 2005 *Phys. Rev.* B **71** 235409–14
[15] Al Salman A, Tortschanoff A, Mohamed M B, Tonti D, van Mourik F and Chergui M 2007 *Appl. Phys. Lett.* **90** 093104–6
[16] Joshi A, Narsingi K Y, Manasreh M O, Davis E A and Weaver B D 2006 *Appl. Phys. Lett.* **89** 131907–9
[17] Gu P, Zhang Y, Feng Y, Zhang T, Chu H, Cui T, Wang Y, Zhao J and Yu W W 2013 *Nanoscale* **5** 10481–6
[18] Liang R, Tian R, Shi W, Liu Z, Yan D, Wei M, Evans D G and Duan X 2013 *Chem. Commun.* **49** 969–71
[19] Sarkar B 2002 *Heavy Metals in the Environment* (Boca Raton, FL: CRC)
[20] Uehara M, Watanabe K, Tajiri Y, Nakamra H and Maeda H 2008 *J. Chem. Phys.* **129** 134709–14
[21] Tan Z *et al* 2011 *Adv. Mater.* **23** 3553–8
[22] Yu W W, Wang Y and Peng X 2003 *Chem. Mater.* **15** 4300–8
[23] Yu W W and Peng X 2002 *Angew. Chem. Int. Ed.* **41** 2368–71
[24] Zhang Y, Dai Q, Li X, Liang J, Colvin V, Wang Y and Yu W W 2011 *Langmuir* **27** 9583–7
[25] Liu W *et al* 2013 *J. Phys. Chem.* C **117** 19288–94
[26] Tran T K C, Le Q P, Nguyen Q L, Li L and Reiss P 2010 *Adv. Nat. Sci.: Nanosci. Nanotechnol.* **1** 025007–11
[27] Li L, Pandey A, Werder D J, Khanal B P, Pietryga J M and Klimov V I 2011 *J. Am. Chem. Soc.* **133** 1176–9
[28] Zhong H, Zhou Y, Ye M, He Y, Ye J, He C, Yang C and Li Y 2008 *Chem. Mater.* **20** 6434–43